

The pancreatic tumor microenvironment of treatment-naïve patients causes a functional shift in $\gamma\delta$ T cells, impairing their anti-tumoral defense

Elena Lo Presti^{a*}, Francesca Cupaioli^{b*}, Daniela Scimeca^c, Elettra Unti^d, Vincenzo Di Martino^e, Rossella Daidone^f, Michele Amata^c, Nunzia Scibetta^d, Erinn Soucie^f, Serena Meraviglia^g, Juan Iovanna^f, Nelson Dusetti^f, Andrea De Gaetano^{a,h,i}, Ivan Merelli^{b#}, and Roberto Di Mitri^{c#}

^aNational Research Council of Italy (CNR), Institute for Biomedical Research and Innovation (IRIB), Palermo, Italy; ^bNational Research Council of Italy, Bioinformatics Research Unit, Institute for Biomedical Technologies Segrate, Milan, Italy; ^cGastroenterology and Endoscopy Unit, Arnas Civico Di Cristina Benfratelli Hospital, Palermo, Italy; ^dAnatomic-pathology Unit, Arnas Civico Di Cristina Benfratelli Hospital, Palermo, Italy; ^eImmunohaematology and Transfusion Medicine Unit, Imperia Hospital ASL1 Imperiese, Imperia, Italy; ^fCancer Research Center of Marseille (CRCM), INSERM, CNRS, Aix-Marseille University, Marseille, France; ^gCentral Laboratory of Advanced Diagnosis and Biomedical Research (CLADIBIOR), University of Palermo, Palermo, Italy; ^hNational Research Council of Italy, Institute for Systems Analysis and Computer Science "A. Ruberti," BioMatLab (Biomathematics Laboratory), Rome, Italy; ⁱDepartment of Mathematics, Mahidol University, Bangkok, Thailand

ABSTRACT

Pancreatic ductal adenocarcinoma (PDAC) presents a unique challenge for researchers due to its late diagnosis caused by vague symptoms and lack of early detection markers. Additionally, PDAC is characterized by an immunosuppressive microenvironment (TME), making it a difficult tumor to treat. While $\gamma\delta$ T cells have shown potential for anti-tumor activity, conflicting studies exist regarding their effectiveness in pancreatic cancer. This study aims to explore the hypothesis that the PDAC TME hinders the anti-tumor capabilities of $\gamma\delta$ T cells through blockade of cytotoxic functions. For this reason, we chose to enroll PDAC treatment-naïve patients to avoid the possibility of therapy modifying the TME. By flow cytometry, our research findings indicate that the presence of $\gamma\delta$ T cells among CD45+ cells in tumor tissue is lower compared to CD66+ cells, but higher than in blood. Circulating V δ 1 T cells exhibit a terminal effector memory phenotype (TEMRA) more than V δ 2 T cells. Interestingly, V δ 1 and V δ 2 T cells appear to be more prevalent at different stages of tumor development. In our *in vitro* culture using conditioned medium derived from Patient-derived organoids (PDOs), we observed a shift in expression markers in $\gamma\delta$ T cells of healthy individuals toward an activation and exhaustion phenotype, as confirmed by scRNA-seq analysis extracted from a public database. A deeper understanding of $\gamma\delta$ T cells in PDAC could be valuable for developing novel therapies aimed at mitigating the impact of the pancreatic tumor microenvironment on this cell population.

ARTICLE HISTORY

Received 24 July 2024
Revised 14 January 2025
Accepted 7 February 2025

KEYWORDS

Fine-needle biopsies; gamma delta T cells; immune checkpoints; immunotherapy; patient derived organoids; PDAC

Background

Pancreatic ductal adenocarcinoma (PDAC) is a deadly form of cancer that is projected to become the second leading cause of cancer-related death in the next decade.¹ One of the challenges with PDAC is the delayed diagnosis due to its vague symptoms and the lack of early diagnostic markers.² The median survival after diagnosis of PDAC is only 4–6 months, primarily due to therapeutic resistance, including resistance to immune checkpoint blockade treatments.^{3,4} This resistance can be attributed to the low immunogenicity of tumor cells, strong tumor immunosuppressive mechanisms, or a combination of both. Emerging evidence suggests that the tumor microenvironment (TME) in PDAC plays a crucial role in cancer initiation, progression, and metastasis development.^{5,6} The TME in PDAC is characterized by a highly fibrotic stroma and significant infiltration of immunosuppressive cell populations such

as tumor-associated macrophages (TAMs), regulatory T cells (Tregs), and myeloid-derived suppressive cells (MDSCs).

At present, PDAC is typically treated with a combination of gemcitabine/nab-paclitaxel or FOLFIRINOX (5-fluorouracil, leucovorin, irinotecan, and oxaliplatin), along with surgery when feasible.⁷ Anyway, despite the use of medications targeting key molecular pathways, there is a lack of diagnostic biomarkers that can predict an effective immunological response.⁸


Cytotoxic T cells within pancreatic cancer are limited due to the fibrotic environment and this limits the ability to study untreated patients where conventional therapy has not influenced the immune populations present.⁹ Therefore, there is an urgent need for practical tools to identify the most appropriate markers for developing new drug treatment strategies.

Both our research and that of other groups have emphasized the importance of $\gamma\delta$ T cells as positive prognostic factors.

CONTACT Elena Lo Presti  elena.lopresti@cnr.it  National Research Council (CNR), Institute for Biomedical Research and Innovation (IRIB), Via Ugo La Malfa, 153, Palermo, 90146, Italy

*Authors share first position.

#Authors share last position.

 Supplemental data for this article can be accessed online at <https://doi.org/10.1080/2162402X.2025.2466301>

© 2025 The Author(s). Published with license by Taylor & Francis Group, LLC.

This is an Open Access article distributed under the terms of the Creative Commons Attribution-NonCommercial License (<http://creativecommons.org/licenses/by-nc/4.0/>), which permits unrestricted non-commercial use, distribution, and reproduction in any medium, provided the original work is properly cited. The terms on which this article has been published allow the posting of the Accepted Manuscript in a repository by the author(s) or with their consent.

However, the situation is more complex, being dependent on cancer type, with distinct differences observed between V δ 1+ and V δ 2+ $\gamma\delta$ T cells.^{10,11} V δ 2 expressing cells, a subset of $\gamma\delta$ T cells primarily present in the circulation, are activated in a major histocompatibility complex-unrestricted manner to carry out their function. They express activating cytotoxic receptors, such as NKG2D, which can detect stress-induced molecules like MIC A/B and UL-16-binding proteins. Conversely, V δ 1 expressing cells are predominantly located in epithelial or mucosal barrier sites. These ligands are typically expressed at low levels in normal cells, but are significantly upregulated in stressed and malignant cells.¹² Despite some conflicting research findings, particularly in pancreatic cancer, regarding their anti-tumor or pro-tumor effects, the importance of $\gamma\delta$ T cells in PDAC is evident.¹³ In healthy individuals, the presence of $\gamma\delta$ T cells in the pancreas is minimal, whereas patients with PDAC exhibit a notable increase in the percentage of $\gamma\delta$ T cells in both tissue and peripheral blood. This increase is more pronounced in tumor tissue compared to blood. In PDAC infiltrating lymphocytes, the frequency of $\gamma\delta$ T cells can range up to 75% of T lymphocytes.¹⁴ Preclinical studies suggest that $\gamma\delta$ T cells in the pancreatic tumor stroma interact with pancreatic stellate cells (PSCs)¹⁵ stimulating the production of IL-6 in PDAC PSCs and ultimately influencing the immunosuppressive tumor microenvironment.¹⁶

Taking into account the plasticity of $\gamma\delta$ T cells,⁶ the immunosuppressive microenvironment of pancreatic tumor, characterized by MDSCs and other cell types, could compromise antitumor defense mechanisms through the release of various mediators into the tumor environment.^{17–19}

Our research aims to demonstrate how the tumor microenvironment, predominantly composed of neutrophils and macrophages, influences the ability of $\gamma\delta$ T cells to adopt a pro-tumorigenic function within the tumor tissue. Our findings challenge previous beliefs about the role of $\gamma\delta$ T cells in pancreatic cancer development and suggest that the tumor microenvironment weakens their anti-tumor capabilities through mechanisms of cellular exhaustion, as evidenced by our study using patient-derived organoids. Furthermore, through the analysis of RNAseq data, we identified two distinct subtypes of V δ 2 T cells with unique transcriptome profiles. Our findings demonstrate a clear transition from subtype “a” to subtype “b”.

Methods

Patient cohort

Patient-derived biological material, such as fine-needle/core biopsies from primary tumors and peripheral blood, was obtained from 11 treatment-naive PDAC patients and 4 patients with non-PDAC, both groups therapy-naive at the moment of the analysis. The collection of tissue material and peripheral blood complied with all relevant institutional/governmental regulations. Informed consent was obtained from all subjects prior to material collection.

The analyzed samples from the cohort were collected during the year 2022–2023. The patients in the cohort had undergone endoscopic ultrasonography (EUS) with fine needle aspiration because they had attended an in-hospital outpatient checkup and

needed a diagnosis for surgical intervention or to initiate therapy. It is difficult to obtain tissue biopsies from the pancreas due to its anatomical position and, moreover, the need to avoid extracting healthy pancreatic tissue. Thus, for comparison, we collected peripheral blood cells with original tumor biopsy specimens (11 PDAC patients) and, after histological screening, we analyzed tissue and blood from the non-PDAC patients (4 patients). Patients were characterized as therapy naive and approaching this exam for the first time. Supplementary Table S1 reports the clinical status of the PDAC patients, and the clinical histological information collected in parallel. Fresh biopsies and peripheral blood of PDAC patients were obtained from the ARNAS Civico-Di Cristina-Benfratelli Hospital, Gastroenterology and Endoscopy Unit, in Palermo, Italy. Patient features are shown in Supplementary Table S1. The study was approved by the local ethics committee in March 2022 (Protocol No. 000398) and was conducted in accordance with the principles of the Declaration of Helsinki. Informed consent was obtained from all patients enrolled in the study.

Isolation of infiltrating and circulating immune cells

Tumor tissue and blood were freshly obtained at the time of endoscopy and transported to the laboratory for processing. Biopsies were minced into small pieces followed digestion with collagenase type IV and DNase [Sigma] for 2 h at 37°C with 5% CO₂. After digestion, the cells extracted and washed twice in incomplete medium [RPMI 1640, Gibco]. Peripheral blood mononuclear cells (PBMCs) were isolated by centrifuge at 2000 rpm for 20 min and washed twice in incomplete medium [RPMI 1640, Gibco].

Flow cytometry analysis

Cells were stained for live/dead discrimination using a Live/Dead Fixable Violet Dead Cell Stain Kit [Invitrogen]. Fc receptor blocking was performed with human immunoglobulin [Sigma, 3 μ g/ml final concentration], followed by surface staining with different fluorochrome-conjugated antibodies to study the composition of the different subpopulations. Conjugated monoclonal antibodies [mAbs] were used to characterize the entire population were as follows: anti-CD3, anti-CD45, anti-V δ 1, anti-V δ 2, anti-CD27, anti-CD45RA, anti-TCR $\gamma\delta$, anti-TIM3, anti-TIGIT, anti-LAG3, anti-NKP46, anti-PD1, anti-CD69, anti-CD25. Expression of surface markers was determined by flow cytometry on a FACSCanto II, FACS Fortessa [BD Biosciences] and analyzed using FlowJo software [BD Biosciences]. For every sample, 100,000 nucleated cells were acquired, and values are expressed as percentage of viable lympho- monocytes, as gated by forward and side scatter, and V δ 1 and V δ 2 were detected using CD3 and CD45 double positive on single-live cells.

Immunohistochemistry

For histological analysis, pancreatic tumor specimens were fixed in 10% neutral buffered formalin, processed, and embedded in paraffin. Slides of formalin-fixed, paraffin-embedded tissues were used to evaluate infiltrating $\gamma\delta$ T cells by immunohistochemistry (IHC). We performed IHC using

antibodies directed against $\gamma\delta$ T cells (Santa Cruz Biotechnology, Clone H-41) as indicated in a recent publication.²⁰ Images were acquired using the Zeiss AxiCam microscope along with AxioVision (Carl Zeiss, Thornwood, New York). The proximity of $\gamma\delta$ T cells to tumor sites was determined by measuring the distance between a $\gamma\delta$ T cell and its spatially closest tumor site at low power fields (20X), and the positivity of the staining was observed at higher power fields (40X).

***In vitro* culture of $\gamma\delta$ T cells with PDAC PDO conditioned medium**

Conditioned medium (CM) from Patient-derived organoids (PDOs) was obtained from three PDAC patients following the methods published by Fraunhofer et al.²¹ PDOs were put in culture for 4 days in filtered Dulbecco's Modified Eagle Medium/Ham's F-12 (DMEM-F12, Gibco) 1X Penicillin-streptomycin (Sigma-Aldrich) and 10% Bovine Serum Albumin (BSA, Sigma-Aldrich). $\gamma\delta$ T cells were enriched from five blood bags from different healthy donors using the MACS Cell Isolation Kit (TCR γ / δ + T Cell Isolation Kit) and autoMACS Pro Separator (Miltenyi Biotec) and after counting they were incubated in 96 well-plates for 1 O.N. in 200 μ l of RPMI or in 200 μ l of CM at the density of 10^6 /ml.²² After incubation, cells were collected, stained, and analyzed as indicated in the flow cytometry section.

Single-cell RNA sequencing and data processing

Data acquisition and preprocessing

scRNA-seq data of 33 PDAC samples (T) and 11 uninvolved (N) tissue from pancreas were downloaded from Sequence Read Archive (SRA), BioProject ID PRJNA806978 (MDA1 and MDA2 dataset) obtaining 22,164 cells.

All datasets were merged in a single object using the R package Seurat (version 4.2.0).²³ This dataset was filtered and cells with a mitochondrial count ratio higher than 10% and < 200 or > 8000 expressed genes were removed. UMI counts were log normalized and scaled for a factor of 10,000. The top 20% of variable genes were selected for downstream analysis. Cell cycle scores were assigned with the CellCycleScoring function using a reference gene lists.²⁴ The number of UMI counts, the percentage of mitochondrial genes, and the differences in cell cycle phases were used to scaled data and regress out unwanted variability. We looked at the difference between the scores for the S phase and the G2/M phase of the cell cycle. Downstream analysis was performed on the top 30 principal components (PCs). The R package Harmony was used to mitigate batch effect and integrate the dataset from different donors²⁵ and RunALRA was used to impute missing or drop-out values.

Gamma delta T cells identification

T cells expressing TRDC, TRGC1 or TRGC2 were annotated as gamma delta (GD) and subset as a separated object of 1,847 cells, on which the previous analysis workflow was repeated. Specific marker genes (CD3G, CD3E, CD3D, CD4, CD8A,

CD8B, TRDC, TRDV1, TRDV2, TRGC1, TRGC2, CD27, PTPRC) (BD Biosciences and Miltenyi Biotec) were plotted to confirm the identity of these cells. UMAP dimensionality reduction and clustering were computed on the top five Harmony corrected principal components. The Louvain algorithm was used to optimize modularity. Downstream analyses were performed on 1.2 clustering resolution.

Cluster biomarkers were identified by FindAllMarkers function setting a logFC threshold of 0.25 and fraction of cells expressing gene greater than 0.2 within one of the two groups. Additionally, Wilcoxon Rank Sum test was applied to identify differentially expressed genes. UCell signature enrichment package²⁶ and AddModuleScore Seurat function were used to highlight custom reference signature and to identify GD cluster subtypes.^{27,28}

Pseudotime

Trajectory inference was analyzed with slingshot package²⁹ as described in the official vignette. GD1 and GD2_a clusters were used as starting point for inferring cellular lineage and pseudotime trajectories.

Differential gene expression

We compared clusters within the same condition using the FindAllMarkers function with a logFC threshold of 0 and return.thresh parameter of 1. Log2FC of selected genes in the different clusters and conditions were represented in a heatmap (ordered by sum of avg log2FC) by using the ggplot2 R package (v3.2.1) and *p* value adjusted was used to determine their significance levels.

Gene Set Enrichment Analysis (GSEA)

We compared clusters between conditions (T vs N) to highlight differences between T-cells expressing GD receptors in tumor and normal tissue, and GD2_b vs GD2_a to investigate the switch of GD2 cells from normal to tumor phenotype using the FindMarkers function. Specifically, clusters with at least three cells were considered for differential gene expression analysis, and a logFC threshold of 0 and return.thresh parameter of 1 were set to output all genes.

Gene Set Enrichment Analysis was performed on the full output marker gene lists by the GSEA function of ClusterProfiler R package⁷⁴ (v3.8.1) focusing on the hallmarks genesetv7.0 (from MSigDB). Results were combined into a single matrix of Normalized Enriched Scores (NES) and graphically represented in a heatmap or barplot by ggplot2 R package (v3.2.1). HALLMARK terms were ranked by sum of NES and *p.adjust* values (less than 0.001, 0.01 and 0.05) underscore the statistical significance of the NES values.

Statistical analyses

Data were analyzed for statistical significance using the paired t-test (Tukey's multiple comparison test) and unpaired Mann-Whitney test for two groups, and the Kruskal-Wallis test for more than two groups. Differences between groups with

a probability of 0.05 were regarded as significant. All data were analyzed using GraphPad Prism version 9 (GraphPad, San Diego, CA). All values are expressed as medians, quartiles, and averages \pm SEM.

Results

Marked heterogeneity in the frequency of $\gamma\delta$ T cells observed in tumor tissue biopsies and peripheral blood samples of PDAC patients

Endoscopic ultrasound-guided fine needle biopsies (EUS-FNBs) have transformed the practice of diagnosing pancreatic adenocarcinoma by replacing surgical biopsies, thus resulting in lower costs, technical ease, and decreased morbidity.³⁰ In this work, we propose to use this procedure for the diagnosis and identification of the immune profile of infiltrating cells, comparing them to circulating cells to propose possible therapeutic interventions.

The frequency of infiltrating and circulating $\gamma\delta$ T cells was analyzed using flow cytometry, following the gating strategy shown in Figure 1a. Our analysis revealed that the enrolled patients exhibited a small percentage of

infiltrating $\gamma\delta$ T cells among CD45+ cells, which was significantly lower compared to activated human CD66b+ granulocytes (Figure 1b). The absolute numbers of $\gamma\delta$ T cells and granulocytes in PDAC patients are not analyzed in this study, but have been reported in other publications, highlighting the importance of monitoring circulating $\gamma\delta$ T cells in PDAC patients.^{31,32} Specifically, we observed that $\gamma\delta$ T cells infiltrated tumor tissue at a median percentage of $2.5\% \pm 3.2$ (median \pm SD), which was significantly higher than in non-PDAC patients. Interestingly, we found that the percentages of circulating V δ 1 T cells ($0.46\% \pm 1.42$) did not differ significantly from those of circulating V δ 2 T cells ($1.4\% \pm 3.1$).

Interestingly, previous studies by Daley and colleagues reported a much higher percentage of $\gamma\delta$ T cells in their samples (around 40%) (13, 22), but our results using the same gating strategy did not align with this finding. Additionally, we observed a notable diversity in the percentages of both V δ 1 and V δ 2 T cells in PDAC patients, with more variability seen in V δ 2 T cells compared to non-PDAC patients (Figure 1c).

In our sample cohort, $\gamma\delta$ T cells were sparsely localized in the PDAC tumor microenvironment as we demonstrated in IHC analysis (Figure 1d), in contrast to previous findings by

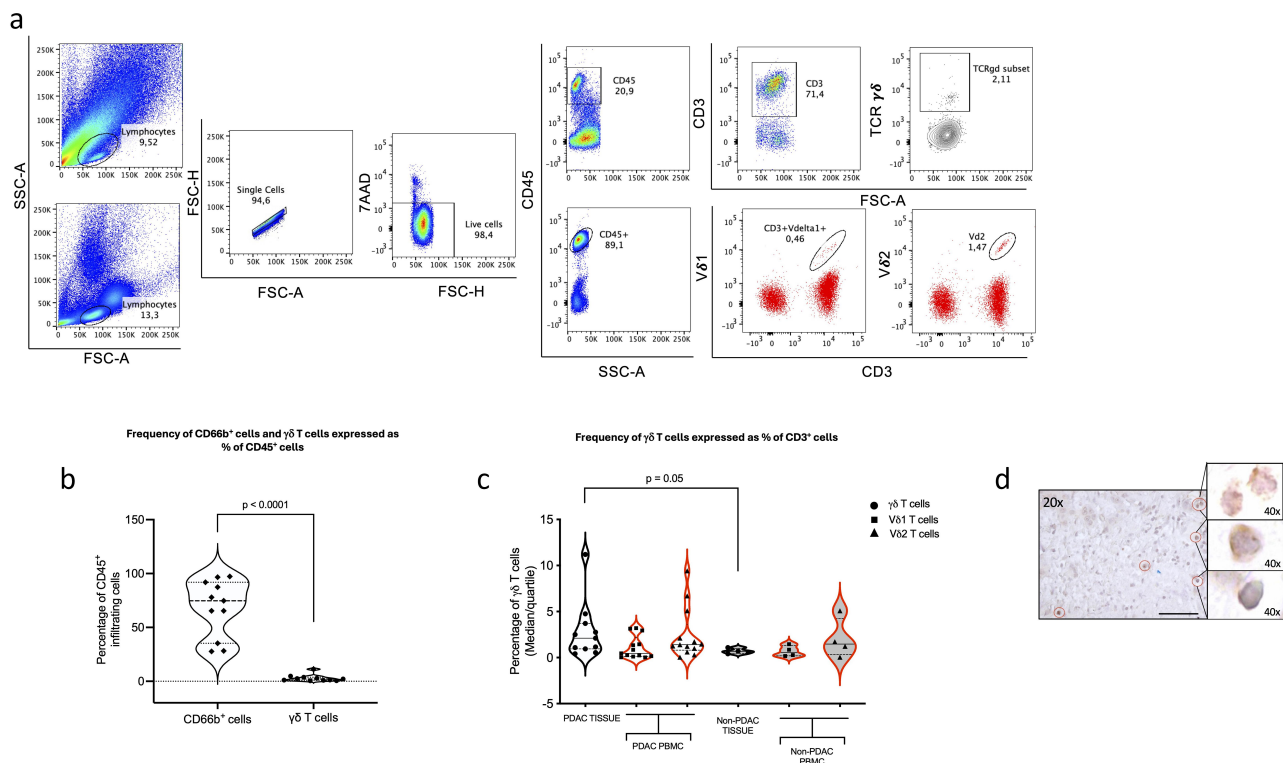


Figure 1. Infiltrating and circulating $\gamma\delta$ T cells show heterogeneous frequencies in PDAC patients compared with non-PDAC patients. a) representative dot plots of PDAC-infiltrating $\gamma\delta$ T cells and circulating V δ 1 and V δ 2 T cells from the same patients, and the relative gating strategies. b) Cumulative graph comparing individual values of infiltrating leukocytes (CD45+ cells) from PDAC patients and, in particular, CD66b+ cells and $\gamma\delta$ TCR+ cells. The analysis of CD66b cells was obtained using the gating strategy reported as follows: SSC-A/FSC-A dot plot > single cells > live cells > CD45+ cells/SSC-A > CD66b+/FSC-A. c) representative violin plots comparing infiltrating (black contour line) and circulating (red contour line) $\gamma\delta$ T cells and their subsets from PDAC patients and non-PDAC patients (gray violin). Black circles indicate $\gamma\delta$ TCR+ T cells, black squares indicate V δ 1 T cells, black triangles indicate V δ 2 T cells. d) Representative paraffin section of human PDAC patients were stained using a mAb specific for TCR $\gamma\delta$. Pictures were acquired with 20X and 40X magnification, the latter was used to evaluate staining specificity. In 20X magnification scale bar represents 100 μ m. 11 PDAC patients and 4 Non-PDAC patients analyzed. Statistical differences were assessed using unpaired student's t-test with Mann-Whitney test, and data are expressed as median (continuous line) and quartiles (dashed lines).

Daley et al.¹⁴ Overall, our data, although collected from a representative number of patients, indicate that $\gamma\delta$ T cells are more abundant in both PDAC tissue and blood compared to non-PDAC patients, underscoring the importance of studying these cells in PDAC patients.

Immunophenotyping analysis of $\gamma\delta$ T cells and their subsets in patients with PDAC showed distinct expression of immunosuppressive markers

It is well established that pancreatic cancer patients exhibit immune dysfunction. The tumor microenvironment (TME) in pancreatic cancer is known to be immunosuppressive, creating an inhibitory environment for the immune system and contributing to the development of highly resistant pancreatic cancer.

To highlight the impact of the pancreatic ductal adenocarcinoma (PDAC) TME on $\gamma\delta$ T cells in treatment-naive patients, we analyzed the phenotypes by using of markers CD45RA and CD27³³ detected on infiltrating $\gamma\delta$ T cells and circulating subsets in these individuals. V δ 1 T cells were predominantly of the terminally differentiated effector memory RA (TEMRA) phenotype, with comparable percentages of other phenotypes. In contrast, V δ 2 T cells exhibited a central memory (CM) phenotype with few effectors memory (EM) cells and did not display a predominance of TEMRA cells (Figure 2a).

In Figure 2b, the relative gating strategy and representative dot plots are shown. Subsequently, we aimed to test our hypothesis that the tumor microenvironment (TME) alters $\gamma\delta$ T cells. We evaluated whether markers related to immunological checkpoints differed between infiltrating and circulating $\gamma\delta$ T cells. Recent publications suggest that TIGIT and TIM3 play a significant role in immune regulation.

In tumor tissue, TIGIT-expressing $\gamma\delta$ T cells exhibited a significantly lower percentage compared to TIGIT-expressing $\gamma\delta$ T cells in non-PDAC tissue (mean \pm SEM 19.3% \pm 7.78 versus 58.3% \pm 25 with ($p < 0.01$)). The variance in frequency of TIM3 in non-PDAC infiltrating $\gamma\delta$ T cells differed from that of PDAC patients (means were 44.50% versus 17.38%) (Figure 2c). Circulating V δ 1 T cells expressed more TIGIT than TIM3 (mean \pm SEM 56.48% \pm 7.9 versus 0.48% \pm 0.26), and this disparity was statistically significant. However, there was no difference between V δ 1 expressing TIGIT and TIM3 in non-PDAC patients. V δ 2 T cells in PDAC patients expressing both TIGIT and TIM3 displayed lower levels compared to non-PDAC patients (mean of: TIGIT-V δ 2 1.07%; TIM3-V δ 2 0.33% versus TIGIT-V δ 2 10.67%; TIM3-V δ 2 4.27%) (Figure 2d,e). Circulating V δ 1 expressing PD1 shown significant high level ($p = 0.03$) than V δ 2 obtained from the same patients (mean \pm SEM 26% SEM 7.2 versus 2.4% SEM 0.46 respectively) (Supplementary data Figure 1a). Additionally, the percentage of V δ 1 expressing CD69 was higher than V δ 2 (Supplementary data Figure 1b)

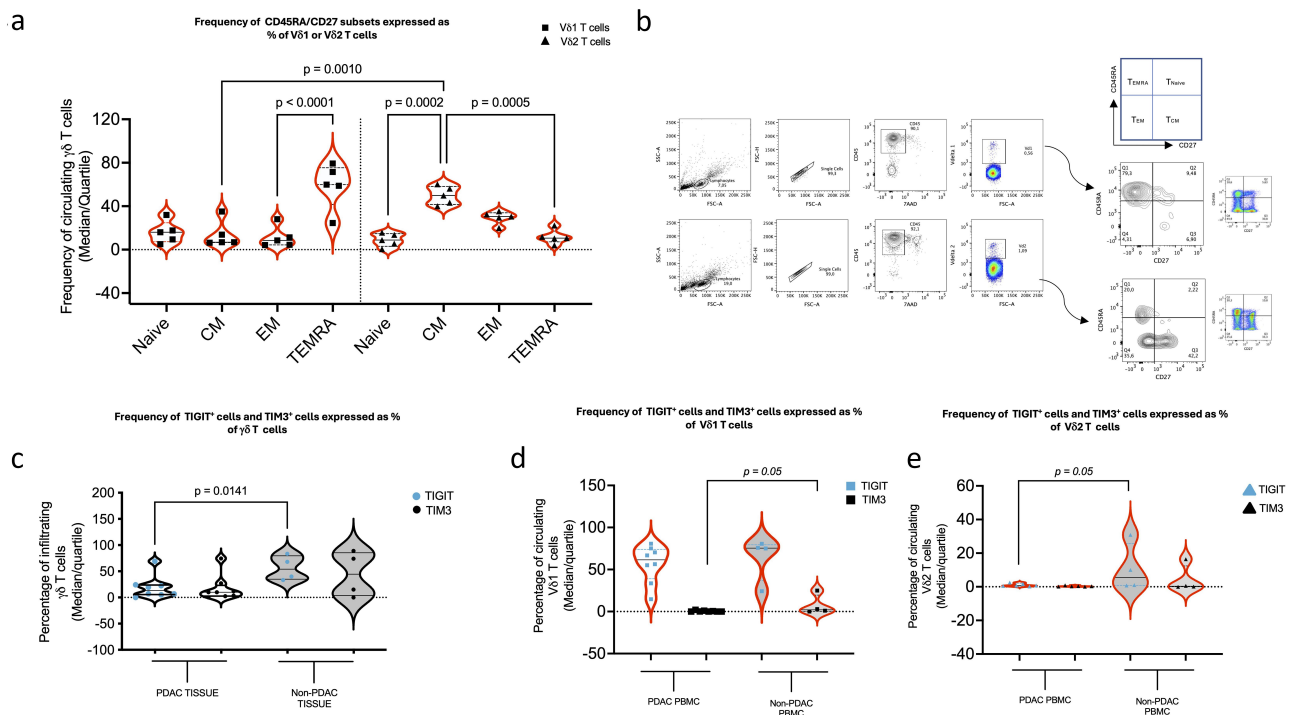


Figure 2. Immunocharacterization of $\gamma\delta$ T cells from tissue and blood of PDAC patients compared to non-PDAC patients show distinctive profiles. a) representative violin plots of the phenotypes of circulating V δ 1 and V δ 2 T cells (red contour line) from PDAC patients (5 samples). Black squares indicate V δ 1 T cells, black triangles indicate V δ 2 T cells. Statistical differences were assessed using one-way ANOVA, Tukey's multiple comparisons test and data are expressed as median (continuous line) and quartiles (dashed lines). b) representative pseudocolor-plots and counter plots of PDAC-circulating V δ 1 and V δ 2 T cells from the same patients and the relative gating strategies. c) representative violin plots of TIGIT+ or TIM3+ infiltrating $\gamma\delta$ T cells (black contour line) and comparing PDAC patients and non-PDAC patients (gray violin) (8 samples PDAC patients and 4 Non-PDAC patients analyzed). d) representative violin plots of TIGIT+ or TIM3+ circulating V δ 1 and V δ 2 T cells (red contour line) and comparing PDAC patients and non-PDAC patients (gray violin) (8 samples PDAC patients and 4 Non-PDAC patients analyzed). e) violin plot comparing NKp46+ $\gamma\delta$ T cells from tissue (black contour line) and blood (red contour line) from PDAC patients (6 samples PDAC patients and 4 Non-PDAC patients analyzed). Statistical differences were assessed using unpaired student's t-test with Mann-Whitney test, and data are expressed as median (continuous line) and quartiles (dashed lines).

and our research revealed that circulating $\gamma\delta$ T cells displayed increased levels of NKp46 compared to infiltrating $\gamma\delta$ T cells (Supplementary data Figure S1c). This indicates that V δ 1 T cells in the circulation possess a more cytotoxic phenotype relative to V δ 2 T cells (see Supplementary Figure S1) and in blood there are more TIGIT-expressing V δ 1 T cells than V δ 2 T cells.

The subsets of $\gamma\delta$ T cells are present in varying proportions among naïve-therapy PDAC patients at different clinical stages

Emerging evidence suggests that tumor-infiltrating immune cells could be used as prognostic markers for various types of cancer. While pancreatic ductal adenocarcinoma (PDAC) is typically poorly infiltrated, we investigated the frequencies of $\gamma\delta$ T cells obtained from tumor tissue (graphs in gray) and circulating subsets (graphs in red) across different tumor stages. As PDAC is often only detected at an advanced stage, our data collection began at Stage II (T2). Treatment-naïve PDAC patients exhibited higher levels of infiltrating $\gamma\delta$ T cells at T2 compared to other stages, although these differences were not statistically significant (Figure 3a). Flow cytometry analysis of $\gamma\delta$ T cells from peripheral blood mononuclear cells (PBMC) showed varying levels of both

V δ 1 and V δ 2 T cells across stages. Circulating V δ 1 T cells were more prevalent at T3 and T4, while V δ 2 T cells were significantly higher in T2 patients compared to V δ 1 T cells (Figure 3b). These findings indicate distinct participation levels of V δ 1 and V δ 2 T cells in tumor immune surveillance.

Furthermore, we evaluated lymph node infiltration, a common feature of advanced tumor stages, to explore the involvement of $\gamma\delta$ T cells in PDAC. Surprisingly, circulating V δ 2 T cells showed significantly higher levels compared to V δ 1 T cells in the N1 stage, with statistically significant data (Figure 3d), despite $\gamma\delta$ T cells not demonstrating a significant correlation in the N1 stage (Figure 3c).

Our findings have confirmed the involvement of $\gamma\delta$ T cells in various stages of tumor development. Additionally, Figure 3e illustrates how we processed data from PDAC patients to stratify them based on clinical and immunological features.

At stage T3, infiltrating $\gamma\delta$ T cells exhibited higher expression of TIGIT and TIM3 compared to other tumor stages (Figure 3f, upper part), and were associated with advanced tumor stages as they were present during stage N2 (Figure 3f, lower part). On the other hand, a greater percentage of TIGIT+V δ 1 T cells and non-TIM3+ V δ 1 T cells were significantly present in T3 patients compared to M1 patients (Figure 3g, upper part), but these were not observed at the advanced stage

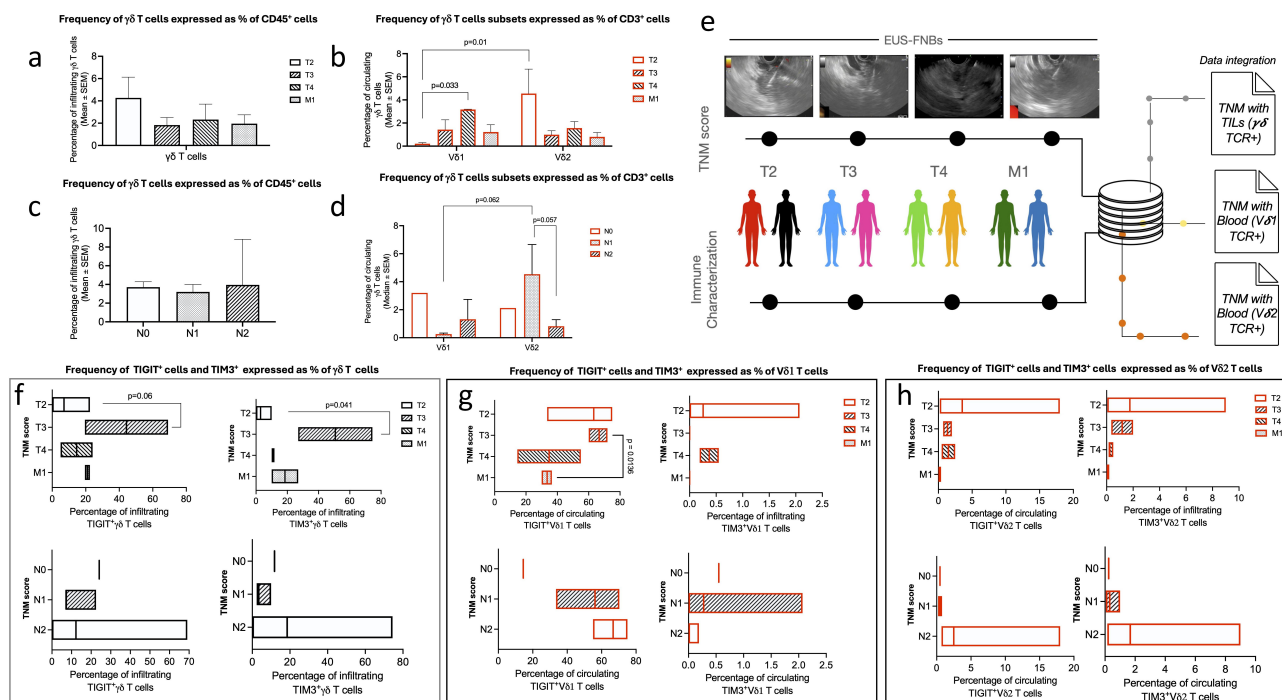


Figure 3. Deep analysis of the expression markers in different clinical tumor stages reveals the early involvement of $\gamma\delta$ T cells subsets. a) representative histogram showing frequency of infiltrating $\gamma\delta$ T cells and b) the circulating subsets of V δ 1 and V δ 2 T cells at different tumor stages (from T2 to T4) and c) and d) of infiltrating lymph nodes (N) classified by TNM score, obtained by flow cytometry analysis. In b) and d) the red contour line indicates the analysis of circulating subsets of $\gamma\delta$ T cells related to the clinical stages. Statistical differences were assessed using unpaired Kruskal-Wallis test, data shown are median and SEM. e) graphical representation of the analysis shown in F-H in which the immune characterization evaluating specific markers expression is correlated with different tumor stages detected by EUS-FNBs and confirmed by pathological anatomy report; f) cumulative box-plot floating bar with minimum and maximum and median as the middle line of TIGIT+ or TIM3+ $\gamma\delta$ T cells from tumor tissue at different tumor stages (black contour line). g) and h) show cumulative data for circulating V δ 1 and V δ 2 (red contour line) with minimum and maximum and median as the middle line. The figures represent the cumulative data of 11 different samples distributed across the various tumor stages. Statistical differences were assessed by using unpaired student's *t*-test with Mann-Whitney test.

N2 (Figure 3g, lower part). There was a distinct distribution of V δ 2 T cells among PDAC patients across different tumor stages, with slightly higher levels at the advanced stage N2 (Figure 3h).

In conclusion, our data suggest that the exhausted phenotype of $\gamma\delta$ T cells and their subsets is associated with advanced tumor stages (T3 and N2), rather than with the metastatic stage. To further validate our findings, we conducted an *in vitro* assay using PDAC PDO.

The analysis of $\gamma\delta$ T cells following *in vitro* culture with PDAC patient-derived organoid conditioned medium demonstrated the significant impact of the pancreatic cancer microenvironment

It has been shown that the function of immune cells, including $\gamma\delta$ T cells, can be altered or hindered by components of the tumor microenvironment (TME). Our study revealed that the TME impairs the function of $\gamma\delta$ T cells, contradicting their expected anti-tumoral role and instead promoting a pro-tumorigenic environment.

By obtaining PDAC PDO (Patient-derived organoid) from fine needle biopsies, we were able to analyze the

communication between T cells and tumor cells *in vitro*. This allowed us to address important questions about the regulation of $\gamma\delta$ T cell function and bridge a crucial gap in research due to the challenges of obtaining biopsies for studying the interactions between immune cells and tumor cells in tumor development.

Using PDAC PDO samples from three different donors, we cultured conditioned media (CM) for an average of 4 days. We then cultured enriched $\gamma\delta$ T cells obtained from blood samples from five different healthy donors in the pooled CM for 24 hours.

Figure 4a depicts the results of the *in vitro* experiment conducted on $\gamma\delta$ T cells in PDAC PDO CM. Various markers associated with T cell functioning and activation were evaluated following *in vitro* culture. TIM3-expressing $\gamma\delta$ T cells (Figure 4b) showed an increase in CM compared to the RPMI control (mean of 3.5% versus 1.57%) and circulating $\gamma\delta$ T cells from PDAC patients (mean of $1.12\% \pm 0.2$ SEM). Furthermore, the analysis of PD1-expressing circulating V δ 1 T cells indicated a statistically significant increase compared to circulating V δ 2 T cells (mean of 25% versus 2.45%) (Supplementary Figure S1a). The analysis revealed that $\gamma\delta$ T cells in PDAC CM

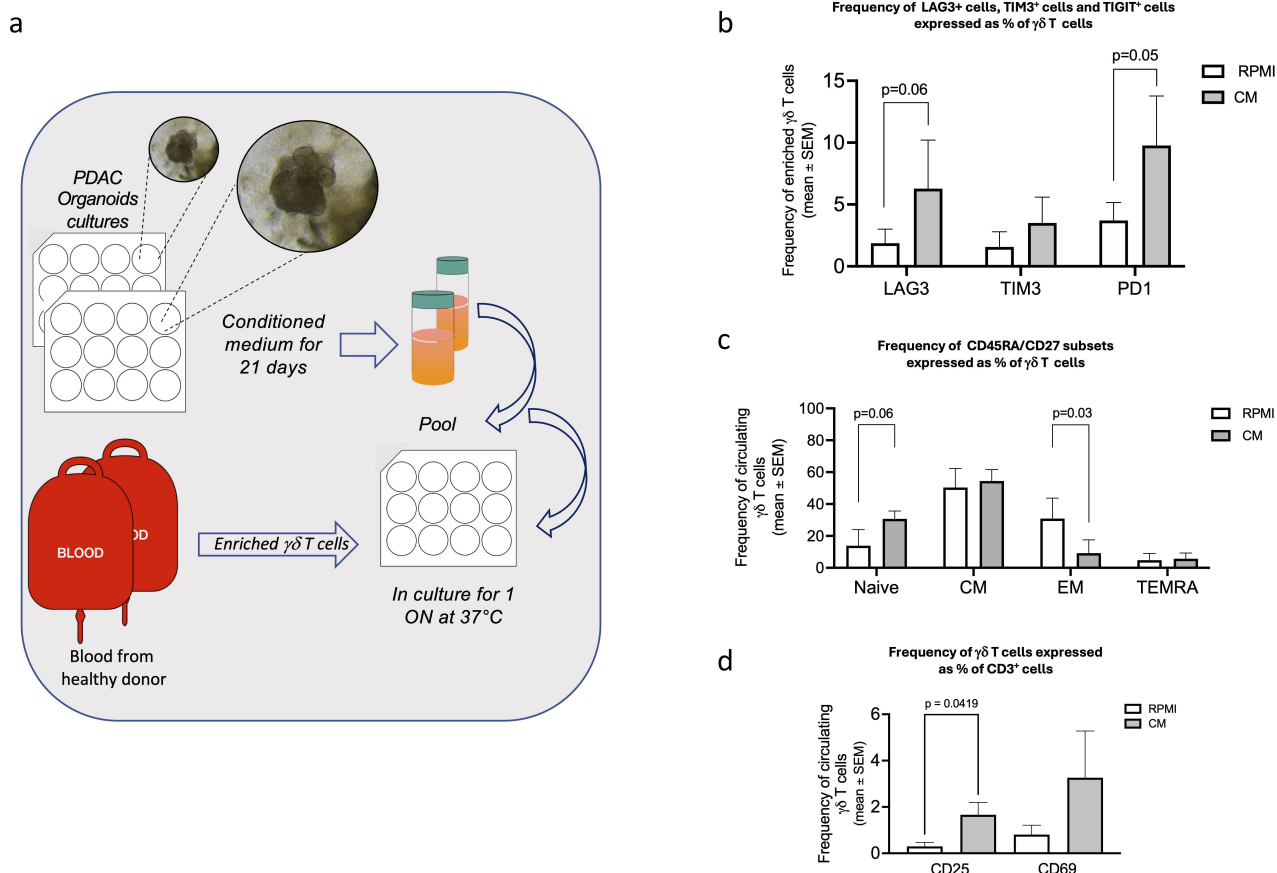


Figure 4. *In vitro* assay demonstrated that PDAC-TME could be selectively responsible for the activation of $\gamma\delta$ T cell subsets and their exhaustion. a) graph illustrating the scheme of the experimental procedure of *in vitro* assays that describes the use of PDAC PDO (from 3 PDAC patients at late stages of tumor) from which we obtained CM after 4 days in culture, and blood from five healthy donors. The experiments were performed putting $\gamma\delta$ T cells in culture 1 on at 37°C and 5% CO₂ with RPMI and in CM, as indicated in material and methods section. b) histogram plot shows median of percentage of TIM3, LAG3 and PD1 expressing $\gamma\delta$ T cells in culture with RPMI (white histogram) and in CM (gray histogram). c) histogram plot shows median of percentage of CD45RA and CD27 expressing $\gamma\delta$ T cells in culture with RPMI (white histogram) and in CM (gray histogram) identifying phenotype. d) histogram plot shows median of percentage of CD25 and CD69 expressing $\gamma\delta$ T cells in culture with RPMI (white histogram) and in CM (gray histogram). Statistical differences were assessed using unpaired student's *t*-test with Mann-Whitney test.

exhibited high levels of CD25 expression (mean of $1.66\% \pm 0.83$ SEM) compared to the RPMI media control (mean of $0.29\% \pm 0.2$ SEM) (Figure 4d). However, the frequency of circulating CD25-expressing $\gamma\delta$ T cells shown a little more expression of CD25 in PDAC patient compared to Non-PDAC patients (Supplementary Figure S1d).

Finally, we aimed to investigate the potential impact of CM from PDAC PDO on the activation of $\gamma\delta$ T cells in treatment-naïve PDAC patients. As anticipated, V δ 1 T cells from the blood of PDAC patients exhibited a significantly higher frequency of CD69 compared to V δ 2 T cells from the same patients (Figure 4d). This finding was consistent with our *in vitro* experiments using PDAC PDO. To validate our theory that PDAC PDO CM can alter cells, we assessed the phenotype using CD45RA and CD27 expression markers. We observed a decrease in the EM phenotype compared to the RPMI control (mean of 30.9% versus 9.1%), which was statistically significant. There were also slightly elevated levels in the TEMRA and naive phenotypes (mean of 13.9% versus 30.7% for the naive phenotype), both with *p* values slightly above 0.05 (Figure 4c). Additionally, the expression of LAG3 and TIM3 on $\gamma\delta$ T cells was increased in the CM culture compared to RPMI (Figure 4b). In conclusion, we found that PDAC tumor cells play a crucial role in modulating the function of $\gamma\delta$ T cells by altering the expression of immunoregulatory markers, as evidenced by our *in vitro* culture experiments with PDAC PDO CM.

The microenvironment of pancreatic cancer alters the transcriptional profile of $\gamma\delta$ T cells

To evaluate the influence of the tumor microenvironment on $\gamma\delta$ T cell function, we analyzed single-cell RNA-seq data from PDAC tissue (tumor tissue) compared to uninvolved pancreatic tissue (normal tissue) previously published in (Schalck et al., 2022). $\gamma\delta$ T cells were identified by the expression of CD3 and TCR δ constant (TRDC) and variable δ (TRDV) regions (Supplementary Figure S2). The subsets of $\gamma\delta$ T cells was re-clustered to investigate $\gamma\delta$ T cells sub-populations. We obtained 1,847 cells expressing V δ 1 and V δ 2 signatures (Supplementary Figure S3). These cells were resolved into six different clusters (Figure 5a-c) based on similarity and gene expression profiling (Figure 5a. The GD cluster encompasses all $\gamma\delta$ T cells that do not express the genes specific to the V δ 1 and V δ 2 clusters, as detailed in the supplementary data. Among these cells 43.4% express V δ 1 and 56.6% express V δ 2 signature (Figure 5e). The V δ 1 (GD1) subset is more abundant in healthy than in affected tissue (about 21% in normal and 16% in tumor). Within V δ 2 (GD2) subset we identified two different clusters showing a differential gene expression profile, which were named as GD2_a and GD2_b. The GD2_a population is slightly enriched in normal tissue (38.3% in normal vs 20% in tumor), while GD2_b cells were found mainly in tumor, in which represents 36.5% of $\gamma\delta$ T cells compared to 10% found in healthy tissue (Figure 5d,e). We computed gene set enrichment analysis (GSEA) by comparing GD2_b to GD2_a (Figure 6a) and the results show that GD2_b cluster is

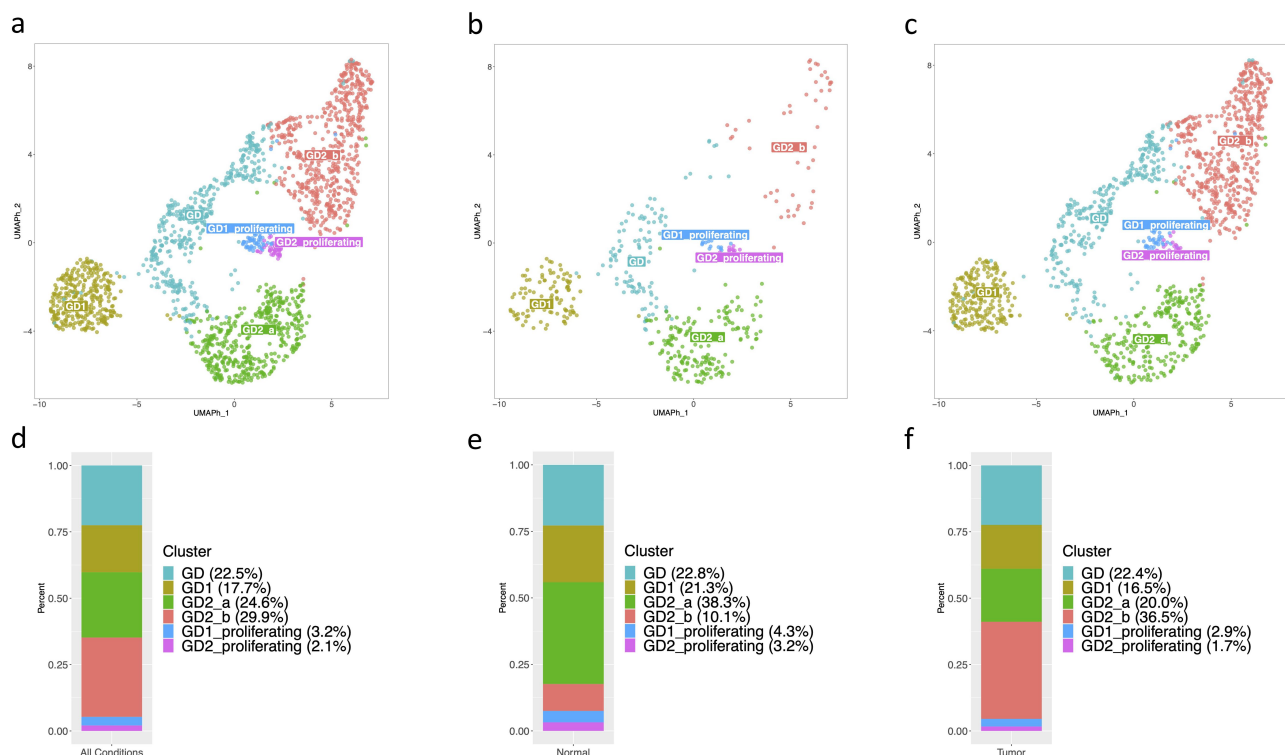


Figure 5. Subpopulations identified in infiltrating $\gamma\delta$ T cells by scRNA transcriptomics. a) UMAP clustering visualization of $\gamma\delta$ T cells subpopulations in the analysis, b) in Normal and c) Tumor tissue. d) Stacked barplot showing the proportion of $\gamma\delta$ T cells subclusters identified in the analysis, e) in Normal and f) in Tumor tissue.

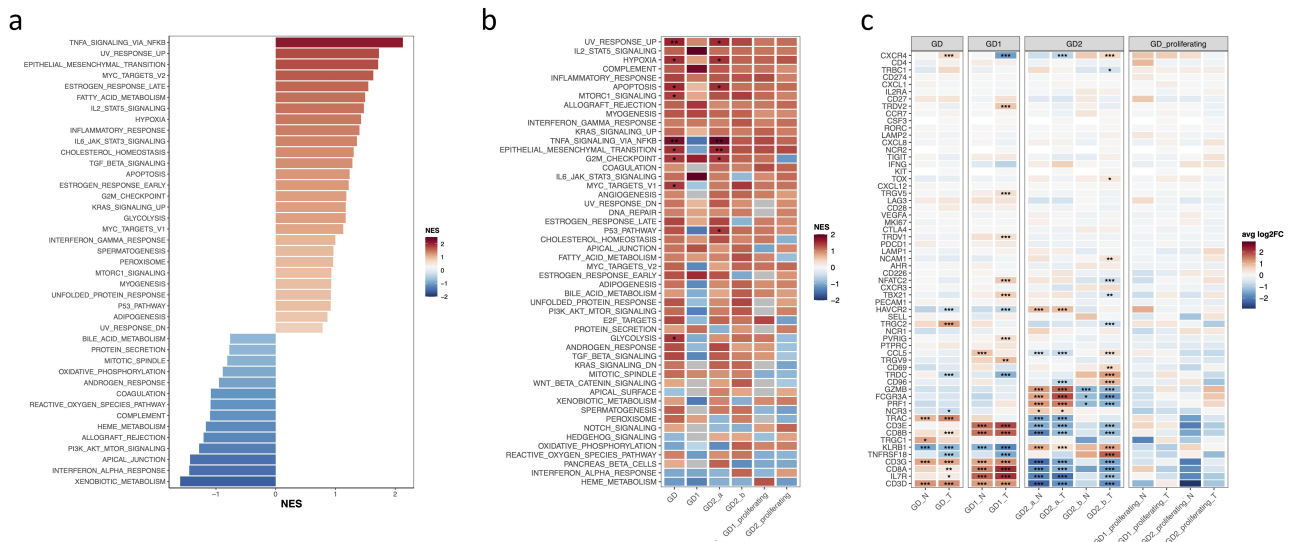


Figure 6. Functional analysis of $\gamma\delta$ T cells subpopulations. GSEA using the Hallmark gene sets in GD2_b vs GD2_a cells (a), and in each cluster within tumor vs normal tissue (b). Tiles are colored according to the Normalized Enrichment Score (NES). c) Expression level of selected genes in each cluster vs all the others within the same condition. Tiles are colored according to the Average logFoldchange (Avg log2FC) and stars were used to indicate the statistical significance ($p < 0.001$ (***), < 0.01 (**), < 0.05 (*)).

characterized by the overexpression of TNF α signaling via NF- κ B signature, proinflammatory genes, hypoxia, fatty acid metabolism and glycolysis pathways. Importantly, the reactive oxygen species pathway, related to protein secretion, is downregulated in the GD2_b cluster in comparison to the GD2_a cluster. Within V δ 1 and V δ 2 T cells we also identified clusters of cells characterized by the overexpression of KRAS signaling signature (Supplementary Figure S4) and we name these cells GD1_proliferating and GD2_proliferating. GD2_proliferating cells are more abundant in normal than in tumor tissue possibly suggesting a decrease in the proliferative capacity of this GD2 subcluster (Figure 5b), but at the same time also a change in the functionality of this subpopulation. Indeed, our research revealed distinct transcriptomic profiles within the $\gamma\delta$ T cell population, indicating the presence of functionally distinct subpopulations, such as GD2_a and GD2_b.

To understand the effect of the tumor microenvironment on the biological functions of $\gamma\delta$ T cells, we performed GSEA comparing each cluster within the two conditions (Figure 6b). We observed that glycolysis, TGF β - pathway, epithelial mesenchymal transition, reactive oxygen species pathways, p53 pathway, unfolded protein response, and TNF α signaling via NF κ B are differentially regulated in GD1 and GD2 cells. In particular, while in the GD1 cluster these pathways are downregulated in tumor, in both the GD2 clusters they are upregulated (Figure 6b). It seems that GD2 undergo a stress related to endoplasmic reticulum which is connected to increase reactive oxygen species with a consequentially inefficacy anti-tumor immune response.

When we analyzed the specific gene expression between GD2_a and GD2_b in normal tissue comparing each cluster to all the others within the same condition (Figure 6c), we found that GD2_b T cells in the tumor poorly expressed genes related to protein secretion, even if they expressed IFN γ and TNF α but the TNFRSF18 gene (member of the

TCR superfamily TNF receptor 18) that play a key role in dominant immunological self-tolerance maintained by regulatory T cells CD25(+)/CD4(+) is up-regulated. Furthermore, granzyme genes in GD2_b in tumor downregulates compared to GD2_a in tumor. NCR3 is less expressed in GD2_b in tumor than in GD2_a in tumor. While CD96, which is a promising candidate for immunotherapy as a novel target of immune checkpoint receptor, is more expressed in GD2_b in tumor than GD2_a in tumor.

We have observed that the CCR5 gene is expressed at lower levels in the GD2_a subset compared to GD2_b in tumor tissue. A similar pattern is seen for the CXCR4 gene, which is known to be upregulated in several cancer types and plays a critical role in tumor metastasis. In multiple sclerosis (MS), a subset of $\gamma\delta$ T cells expressing CCR5 belongs to the effector compartment, supporting the hypothesis that they may contribute to relapse.³⁴ In liver cancer, V δ 2⁺ $\gamma\delta$ T cells predominantly exhibit a CD45RA⁻ CD27⁺ phenotype, with both CCR5 and CD161 generally overexpressed, facilitating their rapid migration to inflammatory tissue.³⁵ $\gamma\delta$ T cell subpopulations in PDAC display unique characteristics that warrant further attention, as these features may provide deeper insights into the true role of $\gamma\delta$ T cells in this tumor.

Finally, we evaluated the possible development of GD1 and GD2 clusters by using a pseudotime analysis including all the conditions (Figure 7). Along the main trajectory of pseudotime, GD tends to enrich in GD2_b in tumor and in GD2_a in normal tissue, with a consequent depletion of GD1 (Figure 7a-d). Moreover, another trajectory can be identified where GD2 cells follow a progression from GD2_a to GD2_b cells when switching from normal tissue to tumor (Figure 7e,f).

These analyses confirm our hypothesis that gamma-delta T cells in the tumor microenvironment exhibit different functional traits compared to those found in normal tissue and acquired in situ, as shown by the pseudotime analyses. Consequently, it is crucial to comprehend these modifications

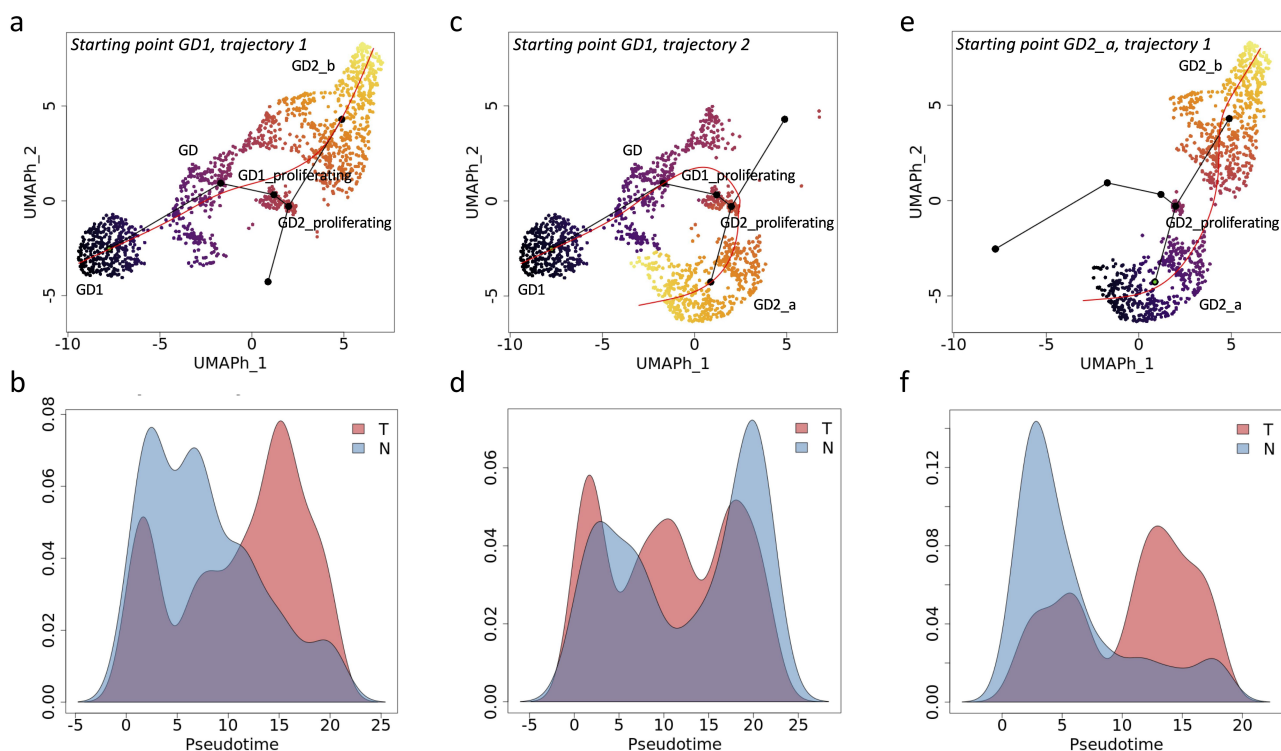


Figure 7. Visualization pseudotemporal trajectory analysis. Pseudotime trajectory analysis and sample density plot of $\gamma\delta$ T cells calculated starting from GD1 (a-d) and GD2_a (e,f) clusters. A color gradient from black to yellow represents different pseudotime levels, with black indicating the earliest time point and yellow indicating the latest time point (a,c,e). Density plots represent the distribution of cells in normal and tumor conditions along the pseudotime (b, d, f). In the transition from normal to tumor microenvironment, GD1 cells are distributed along the trajectory to GD2_b cells (a), as do GD2_a (c). Additionally, GD1 and GD2_a are distributed along the same trajectory in a bidirectional manner (b).

for the advancement of therapies designed to prevent these alterations.

Discussion

We conducted a comprehensive analysis of baseline circulating and infiltrating $\gamma\delta$ T cells in treatment-naïve PDAC patients. Using flow cytometry and an *in vitro* PDAC PDO assay, we examined the immunophenotype of $\gamma\delta$ T cells and their subsets in both peripheral blood and tumor tissue, categorizing these findings based on the patients' clinical stages. Furthermore, we established an *in vitro* culture assay using the conditioned medium of PDAC PDOs derived from three different patients. A key strength of our study lies in the utilization of needle PDAC biopsies of treatment-naïve patients to generate PDAC PDOs, enabling us to analyze infiltrating lymphocytes concurrently with peripheral blood samples from the same patients. Through the use of EUS-FNB, we can provide more accurate prognostic information and tumor classification markers for improved clinical management, facilitating the timely initiation of appropriate therapies while minimizing unnecessary procedures.³⁶

Our research focused on tumor infiltrating $\gamma\delta$ T cells due to their significant prognostic value in various types of human cancer.^{8,13} These cells have shown promise in anti-tumor immune therapy approaches.³⁷ However, studies have also indicated that in the context of pancreatic tumors, $\gamma\delta$ T cells may have tumor-promoting functions.¹⁵ The cytotoxicity

displayed by $\gamma\delta$ T cells against tumors may potentially switch to a supportive role in tumor development.

Interestingly, there was a significant difference in tumor-infiltrating $\gamma\delta$ T cell values between PDAC and non-PDAC control samples, but no difference was observed in the circulating V δ 1 and V δ 2 T cell levels between PDAC and non-PDAC patients. Additionally, we found that the V δ 2 subset was more prevalent than V δ 1 T cells in the blood, although the difference was not statistically significant.

Gene expression data revealed an emerging proliferating V δ 1 population in the tumor compared to the V δ 2 subset, which could support the hypothesis of a tissue-specific presence of V δ 1 cells. However, we acknowledge the lack of flow cytometry data to directly confirm this.

We have suggested that the function of $\gamma\delta$ T cells can be altered or hindered by components in the tumor microenvironment (TME). The presence of $\gamma\delta$ T cells within pancreatic ductal adenocarcinoma (PDAC) infiltrating lymphocytes is variable, as well as the levels found in the bloodstream. A study involving knockout mice revealed that $\gamma\delta$ T cells play a pro-tumorigenic role in PDAC.¹⁴ However, inhibitory factors within the tumor environment inhibit the cytotoxicity of $\gamma\delta$ T cells, leading to weakened antitumor defense mechanisms.³⁸ Our research indicates that $\gamma\delta$ infiltrates in PDAC exhibit fewer immune checkpoints compared to the bloodstream, with a higher proportion of exhausted and cytotoxic V δ 1 T cells compared to V δ 2. We identified two distinct subtypes of V δ 2 lymphocytes, termed GD2_a and GD2_b, with varying gene profiles in normal

and tumor tissues. The presence of these subpopulations suggests a functional switch, as GD2_a retains anti-tumor characteristics while GD2_b shows Treg-like phenotypes. Identifying these subtypes using flow cytometry or immunofluorescence analysis poses a challenge, but as of now, this information remains elusive. The pseudotime analysis of one of the two evaluated trajectories surprisingly reveals that V δ 1 T cells in the tumor tissue are replaced by V δ 2 T cells with a type 2 function. While there is a risk of incorrect clustering that cannot be directly assessed, the ultimate solution requires 5' scRNAseq chemistry datasets to include measurements of all TCRV δ and TCR γ genes, which are not currently implemented. Therefore, there is currently no way to differentiate between TCRV γ 9/TCRV δ 2, TCRV γ 9/TCRV δ non2, TCRV γ non9/TCRV δ 1, and TCRV γ non9/TCRV γ non1, other than simple binary classification into the TCRV γ 9 and TCRV γ non9 groups. To address this limitation, we utilized a gene cluster published by Satija et al. in 2015²³ to group our subsets more effectively. This approach revealed distinct subtypes within the V δ 2 subsets with unique transcriptomic profiles, indicating various responses to microenvironmental influences on recruited $\gamma\delta$ T cells.

Our research indicates that infiltrating $\gamma\delta$ T cells are correlated with LN infiltration, particularly V δ 2 T cells show a correlation with early tumor stages compared to V δ 1 T cells, with statistically significant data. Further exploration of the subtypes of V δ 2 cells, specifically type a or type b, at the LN level would be intriguing; however, we currently lack the ability to have this information. Exploring how the tumor microenvironment affects $\gamma\delta$ T lymphocytes, we conducted an *in vitro* test using PDAC PDO to better understand functional changes induced by the tumor microenvironment. Indeed, we observed that peripheral blood $\gamma\delta$ T cells from healthy individuals, when cultured with PDAC organoid supernatant, exhibit exhaustion markers and a phenotype similar to our *ex-vivo* findings from drug-naive PDAC patient biopsies. Additionally, we found that genes essential for cytotoxic functions are more downregulated in V δ 2 compared to V δ 1.

Although it has been shown that CD8+ T cells in proximity to PDAC cells correlate with increased survival,³⁹ memory CD8+ T cells were less frequent in pancreatic cancers in comparison to nonmalignant pancreatic tissue.⁴⁰ To investigate this issue for $\gamma\delta$ T cells, we evaluated the phenotype using an *in vitro* culture with CM of PDAC PDO. Unfortunately, no strong changes were found in the phenotype of $\gamma\delta$ T cells, except for naive and EM phenotypes, compared to RPMI control. In conclusion, our findings demonstrate that $\gamma\delta$ T cells control tumor progression until the TME does not modify the expression of those markers that control immunosuppressive processes, and this hypothesis seems to be confirmed by scRNAseq analysis.

Unfortunately, a limitation of our study is the small sample size, which reflects the challenge of recruiting treatment-naive patients. However, the inclusion of patients who had not received therapy before is a significant advantage for immunological studies, as recent research has shown that therapy can alter the tumor microenvironment.⁴¹ Furthermore, the presence of $\gamma\delta$ T cells in pancreatic ductal adenocarcinoma (PDAC) infiltrating lymphocytes varies. Not all samples

showed a percentage of $\gamma\delta$ T cells. Due to the low number of cells collected from tumor biopsies, we chose to only stain for $\gamma\delta$ T cells, as outlined in the Materials and Methods section. However, the issue related to the small sample size, was mitigated by conducting *in silico* analyses on a larger cohort of patients than those available for *ex vivo* analysis.

Conclusion

The tumor microenvironment (TME) has been shown to impact the anti-tumor activity of $\gamma\delta$ T cells by weakening and suppressing their cytotoxic mechanisms. The observation of two subtypes of V δ 2 T lymphocytes indicates that there is differentiation over time. While acknowledging the limitations of our study, we advocate for further research to identify strategies that can prevent functional changes in $\gamma\delta$ T cells within the pancreatic cancer microenvironment. This could pave the way for the development of new technologies based on allogeneic $\gamma\delta$ T cell therapy.

Acknowledgments

The authors would like to thank Prof. Francesco Dieli, University of Palermo, for training Elena Lo Presti at University Hospital, “P. Giaccone” in Palermo. We thank Prof. Sebastiano Gangemi at University of Messina, Prof. Manfredi Rizzo at University Hospital, “P. Giaccone” in Palermo, and Prof. Francesco Dieli for support Elena Lo Presti in her research activity.

Disclosure statement

No potential conflict of interest was reported by the author(s).

Funding

This research was funded by Dr. Elena Lo Presti, PNC-PNRR 3D4H project, Project Code: PNC0000001.

Authors' contributions

Conceptualization: ELP and RDM. Resources: DS, VDM, MA, RDM (patients), SM (FACS Canto II), ES, ND, JI (PDAC PDO), RD (References management), IM, FC (PDAC database), EU and NS (formalin-fixed paraffin-embedded tissues). Data curation: ELP, VDM, FC. Formal analysis: ELP (*ex-vivo* and *in vitro* analysis), FC (*in silico* analysis). Supervision: ADG, RDM, NS, JI, IM. Methodology: ELP, ES, IM. Writing-original draft: ELP, FC, IM. Project administration: ELP, DS (clinical support). Writing-review and editing: ELP, FC, DS, VDM, EU, RD, MA, SM, ES, NS, MR, JI, ADG, IM, RDM.

Data availability statement

All data generated or analyzed during this study are included in this published article.

Ethics approval and consent to participate

Ethical committee that approved the study is “Ethical Committee Palermo 2” and the committee's reference number is 000398-Palermo (Italy).

Ethics approval statement

This study was approved by the Ethical Committee of the ARNAS Civico Hospital of Palermo in March 2022 (Protocol No. 000398).

Patient consent statement

Written informed consent for data collection was obtained from all participants in the study.

ORCID

Elena Lo Presti  <http://orcid.org/0000-0001-5401-4545>

References

- Rahib L, Smith BD, Aizenberg R, Rosenzweig AB, Fleshman JM, Matrisian LM. Projecting cancer incidence and deaths to 2030: the unexpected burden of thyroid, liver, and pancreas cancers in the United States. *Cancer Res.* 2014;74(11):2913–2921. doi:10.1158/0008-5472.CAN-14-0155.
- Costello E, Greenhalf W, Neoptolemos JP. New biomarkers and targets in pancreatic cancer and their application to treatment. *Nat Rev Gastroenterol Hepatol.* 2012;9(8):435–444. doi:10.1038/nrgastro.2012.119.
- Foucher ED, Ghigo C, Chouaib S, Galon J, Iovanna J, Olive D. Pancreatic ductal adenocarcinoma: a strong imbalance of good and bad immunological cops in the tumor microenvironment. *Front Immunol.* 2018;9:1044. doi:10.3389/fimmu.2018.01044.
- Binnewies M, Roberts EW, Kersten K, Chan V, Fearon DF, Merad M, Coussens LM, Gabrilovich DI, Ostrand-Rosenberg S, Hedrick CC, et al. Understanding the tumor immune microenvironment (TIME) for effective therapy. *Nat Med.* 2018;24(5):541–550. doi:10.1038/s41591-018-0014-x.
- Chong YP, Peter EP, Lee FJM, Chan CM, Chai S, Ling LPC, Tan EL, Ng SH, Masamune A, Ghafar SAA, et al. Conditioned media of pancreatic cancer cells and pancreatic stellate cells induce myeloid-derived suppressor cells differentiation and lymphocytes suppression. *Sci Rep.* 2022;12(1):12315. doi:10.1038/s41598-022-16671-9.
- Siret C, Collignon A, Silvy F, Robert S, Cheyrol T, André P, Rigot V, Iovanna J, van de Pavert S, Lombardo D, et al. Deciphering the crosstalk between myeloid-derived suppressor cells and regulatory T cells in pancreatic ductal adenocarcinoma. *Front Immunol.* 2019;10:3070. doi:10.3389/fimmu.2019.03070.
- Von Hoff DD, Ervin T, Arena FP, Chiorean EG, Infante J, Moore M, Seay T, Tjulandin SA, Ma WW, Saleh MN, et al. Increased survival in pancreatic cancer with nab-paclitaxel plus gemcitabine. *N Engl J Med.* 2013;369(18):1691–1703. doi:10.1056/NEJMoa1304369.
- Tosolini M, Pont F, Poupot M, Vergez F, Nicolau-Travers M-L, Vermijlen D, Sarry JE, Dieli F, Fournié J-J. Assessment of tumor-infiltrating TCRV γ 9V δ 2 $\gamma\delta$ lymphocyte abundance by deconvolution of human cancers microarrays. *OncoImmunology.* 2017;6(3):e1284723. doi:10.1080/2162402X.2017.1284723.
- Lo Presti E, Mocciano F, Mitri RD, Corsale AM, Di Simone M, Vieni S, Scibetta N, Unti E, Dieli F, Meraviglia S, et al. Analysis of colon-infiltrating $\gamma\delta$ T cells in chronic inflammatory bowel disease and in colitis-associated cancer. *J Leukoc Biol.* 2020;108(2):749–760. doi:10.1002/JLB.5MA0320-201RR.
- Mensurado S, Blanco-Domínguez R, Silva-Santos B. The emerging roles of $\gamma\delta$ T cells in cancer immunotherapy. *Nat Rev Clin Oncol.* 2023;20(3):178–191. doi:10.1038/s41571-022-00722-1.
- Meraviglia S, Lo Presti E, Dieli F, Stassi G. $\gamma\delta$ T cell-based anticancer immunotherapy: progress and possibilities. *Immunotherapy.* 2015;7(9):949–951. doi:10.2217/imt.15.68.
- Nezhad Shamohammadi F, Yazdanifar M, Oraei M, Kazemi MH, Roohi A, Mahya Shariat Razavi S, Rezaei F, Parvizpour F, Karamlou Y, Namdari H, et al. Controversial role of $\gamma\delta$ T cells in pancreatic cancer. *Int Immunopharmacol.* 2022;108:108895. doi:10.1016/j.intimp.2022.108895.
- Chabab G, Boissière-Michot F, Mollevi C, Ramos J, Lopez-Crapez E, Colombo P-E, Jacot W, Bonnefoy N, Lafont V. Diversity of tumor-infiltrating, $\gamma\delta$ T-cell abundance in solid cancers. *Cells.* 2020;9(6):1537. doi:10.3390/cells9061537.
- Daley D, Zambirinis CP, Seifert L, Akkad N, Mohan N, Werba G, Barilla R, Torres-Hernandez A, Hundeyin M, Mani VRK, et al. $\gamma\delta$ T cells support pancreatic oncogenesis by restraining $\alpha\beta$ T cell activation. *Cell.* 2016;166(6):1485–1499.e15. doi:10.1016/j.cell.2016.07.046.
- Seifert AM, List J, Heiduk M, Decker R, von Renesse J, Meinecke A-C, Aust DE, Welsch T, Weitz J, Seifert L, et al. Gamma-delta T cells stimulate IL-6 production by pancreatic stellate cells in pancreatic ductal adenocarcinoma. *J Cancer Res Clin Oncol.* 2020;146(12):3233–3240. doi:10.1007/s00432-020-03367-8.
- Seifert AM, Reiche C, Heiduk M, Tannert A, Meinecke A-C, Baier S, von Renesse J, Kahlert C, Distler M, Welsch T, et al. Detection of pancreatic ductal adenocarcinoma with galectin-9 serum levels. *Oncogene.* 2020;39(15):3102–3113. doi:10.1038/s41388-020-1186-7.
- Veglia F, Sanseviero E, Gabrilovich DI. Myeloid-derived suppressor cells in the era of increasing myeloid cell diversity. *Nat Rev Immunol.* 2021;21(8):485–498. doi:10.1038/s41577-020-00490-y.
- Stromnes IM, Brockenbrough JS, Izeradjene K, Carlson MA, Cuevas C, Simmons RM, Greenberg PD, Hingorani SR. Targeted depletion of an MDSC subset unmasks pancreatic ductal adenocarcinoma to adaptive immunity. *Gut.* 2014;63(11):1769–1781. doi:10.1136/gutjnl-2013-306271.
- Coffelt SB, Kersten K, Doornebal CW, Weiden J, Vrijland K, Hau C-S, Verstegen NJM, Ciampricotti M, Hawinkels LJAC, Jonkers J, et al. IL-17-producing $\gamma\delta$ T cells and neutrophils conspire to promote breast cancer metastasis. *Nature.* 2015;522(7556):345–348. doi:10.1038/nature14282.
- Jungbluth AA, Frosina D, Fayad M, Pulitzer MP, Dogan A, Busam KJ, Imai N, Gnjatic S. Immunohistochemical detection of $\gamma\delta$ T lymphocytes in formalin-fixed paraffin-embedded tissues. *Appl Immunohistochem Mol Morphol.* 2019;27(8):581–583. doi:10.1097/PAI.0000000000000650.
- Fraunhoffer NA, Abuelafia AM, Bigonnet M, Gayet O, Roques J, Telle E, Santofimia-Castaño P, Borrello MT, Chuluyan E, Dusetti N, et al. Evidencing a pancreatic ductal adenocarcinoma subpopulation sensitive to the proteasome inhibitor carfilzomib. *Clin Cancer Res.* 2020;26(20):5506–5519. doi:10.1158/1078-0432.CCR-20-1232.
- Meraviglia S, Lo Presti E, Tosolini M, La Mendola C, Orlando V, Todaro M, Catalano V, Stassi G, Cicero G, Vieni S, et al. Distinctive features of tumor-infiltrating $\gamma\delta$ T lymphocytes in human colorectal cancer. *Oncoimmunology.* 2017;6(10):e1347742. doi:10.1080/2162402X.2017.1347742.
- Satija R, Farrell JA, Gennert D, Schier AF, Regev A. Spatial reconstruction of single-cell gene expression. *Nat Biotechnol.* 2015;33(5):495–502. doi:10.1038/nbt.3192.
- Kowalczyk MS, Tirosh I, Heckl D, Rao TN, Dixit A, Haas BJ, Schneider RK, Wagers AJ, Ebert BL, Regev A, et al. Single-cell RNA-seq reveals changes in cell cycle and differentiation programs upon aging of hematopoietic stem cells. *Genome Res.* 2015;25(12):1860–1872. doi:10.1101/gr.192237.115.
- Korsunsky I, Millard N, Fan J, Slowikowski K, Zhang F, Wei K, Baglaenko Y, Brenner M, Loh P-R, Raychaudhuri S, et al. Fast, sensitive and accurate integration of single-cell data with harmony. *Nat Methods.* 2019;16(12):1289–1296. doi:10.1038/s41592-019-0619-0.
- Andreatta M, Carmona SJ. Ucell: robust and scalable single-cell gene signature scoring. *Comput Struct Biotechnol J.* 2021;19:3796–3798. doi:10.1016/j.csbj.2021.06.043.
- Sanz M, Mann BT, Ryan PL, Bosque A, Pennington DJ, Hackstein H, Soriano-Sarabia N. Deep characterization of human

- $\gamma\delta$ T cell subsets defines shared and lineage-specific traits. *Front Immunol.* 2023;14:14. doi:10.3389/fimmu.2023.1148988.
28. McMurray JL, von Borstel A, Taher TE, Syrimi E, Taylor GS, Sharif M, Rossjohn J, Remmerswaal EBM, Bemelman FJ, Vieira Braga FA, et al. Transcriptional profiling of human V δ 1 T cells reveals a pathogen-driven adaptive differentiation program. *Cell Rep.* 2022;39(8):110858. doi:10.1016/j.celrep.2022.110858.
 29. Street K, Rizzo D, Fletcher RB, Das D, Ngai J, Yosef N, Purdom E, Dudoit S. Slingshot: cell lineage and pseudotime inference for single-cell transcriptomics. *BMC Genomics.* 2018;19(1):477. doi:10.1186/s12864-018-4772-0.
 30. Eltoum IA, Alston EA, Roberson J. Trends in pancreatic pathology practice before and after implementation of endoscopic ultrasound-guided fine-needle aspiration: an example of disruptive innovation effect? *Arch Pathol Lab Med.* 2012;136(4):447–453. doi:10.5858/arpa.2011-0218-OA.
 31. Tulyte S, Characiejus D, Matuzeviciene R, Janiulioniene A, Radzevicius M, Jasiunaite E, Zvirblis T, Sileikis A. Prognostic value of circulating T-lymphocyte subsets in advanced pancreatic cancer patients treated with mFOLFIRINOX or gemcitabine. *Int Immunopharmacol.* 2023;115:109722. doi:10.1016/j.intimp.2023.109722.
 32. Oberg H-H, Grage-Griebenow E, Adam-Klages S, Jerg E, Peipp M, Kellner C, Petrick D, Gonnermann D, Freitag-Wolf S, Röcken C, et al. Monitoring and functional characterization of the lymphocytic compartment in pancreatic ductal adenocarcinoma patients. *Pancreatology.* 2016;16(6):1069–1079. doi:10.1016/j.pan.2016.07.008.
 33. Dieli F, Poccia F, Lipp M, Sireci G, Caccamo N, Di Sano C, Salerno A. Differentiation of effector/memory V δ 2 T cells and migratory routes in lymph nodes or inflammatory sites. *J Exp Med.* 2003;198(3):391–397. doi:10.1084/jem.20030235.
 34. Monteiro A, Cruto C, Rosado P, Martinho A, Rosado L, Fonseca M, Paiva A. Characterization of circulating gamma-delta T cells in relapsing vs remission multiple sclerosis. *J Neuroimmunol.* 2018;318:65–71. doi:10.1016/j.jneuroim.2018.02.009.
 35. Yin K-L, Chu K-J, Li M, Duan Y-X, Yu Y-X, Kang M-Q, Fu D, Liao R. Immune regulatory networks and therapy of $\gamma\delta$ T cells in liver cancer: recent trends and advancements. *J Clin Transl Hepatol.* 2024;12(3):287–297. doi:10.14218/JCTH.2023.00355.
 36. Hébert-Magee S. Is there a role for endoscopic ultrasound-guided fine-needle biopsy in pancreatic cancer? *Endoscopy.* 2015;47(4):291–292. doi:10.1055/s-0034-1391441.
 37. Paijens ST, Vledder A, de Bruyn M, Nijman HW. Tumor-infiltrating lymphocytes in the immunotherapy era. *Cell Mol Immunol.* 2021;18(4):842–859. doi:10.1038/s41423-020-00565-9.
 38. Gonnermann D, Oberg H-H, Kellner C, Peipp M, Sebens S, Kabelitz D, Wesch D. Resistance of cyclooxygenase-2 expressing pancreatic ductal adenocarcinoma cells against $\gamma\delta$ T cell cytotoxicity. *OncoImmunology.* 2015;4(3):e988460. doi:10.4161/2162402X.2014.988460.
 39. Carstens JL, Correa de Sampaio P, Yang D, Barua S, Wang H, Rao A, Allison JP, LeBleu VS, Kalluri R. Spatial computation of intratumoral T cells correlates with survival of patients with pancreatic cancer. *Nat Commun.* 2017;8(1):15095. doi:10.1038/ncomms15095.
 40. Brouwer TP, de Vries NL, Abdelaal T, Krog RT, Li Z, Ruano D, Fariña A, Lelieveldt BPF, Morreau H, Bonsing BA, et al. Local and systemic immune profiles of human pancreatic ductal adenocarcinoma revealed by single-cell mass cytometry. *J Immunother Cancer.* 2022;10(7):e004638. doi:10.1136/jitc-2022-004638.
 41. Werba G, Weissinger D, Kawaler EA, Zhao E, Kalfakakou D, Dhara S, Wang L, Lim HB, Oh G, Jing X, et al. Single-cell RNA sequencing reveals the effects of chemotherapy on human pancreatic adenocarcinoma and its tumor microenvironment. *Nat Commun.* 2023;14(1):797. doi:10.1038/s41467-023-36296-4.